K. R. Diller
Associate Professor of Mechanical Engineering and Biomedical Engineering, Bio-Heat Transfer Laboratory, Department of Mechanical Engineering, Mem. ASME

L. J. Hayes
Associate Professor of Aerospace Engineering and Engineering Mechanics, Texas Institute for Computational Mechanics.

The University of Texas at Austin, Austin, Tex. 78712

A Finite Element Model of Burn Injury in Blood-Perfused Skin

The burn process resulting from the application of a hot, cylindrical source to the skin surface was modeled using the finite element technique. A rotationally symmetric 125-element mesh was defined within the tissue beneath and outlying to an applied heating disk. The disk temperature and duration of contact were varied, respectively, between 50 and 100°C for up to 30 s. Natural convection with ambient air was assumed for areas of skin surface not in direct contact with the disk. The simulated thermal history was used in a damage integral model to calculate the extent and severity of injury in the radial and axial dimensions.

Background

A thermal burn results from an elevation in tissue temperature above a threshold value for a finite period of time. Both the absolute temperature and the duration of exposure are crucial in determining the extent of injury; the transient tissue temperature integrated as an exponential function over the time of exposure governs the creation of a thermal lesion. The larger the value of this coupled integral, the greater is the potential for injury.

The most frequent cause of skin burns is associated with the surface application of a heat source, whether it be by a conduction, convection, or radiation mode or a combination thereof. Since heat transport from the surface to interior regions is limited by the effective thermal diffusivity of the tissue, a three-dimensional temperature field is established in which significant gradients may exist. Consequently, the temperature history throughout the affected tissue is nonuniform and regions of graded injury develop with the most acute involvement closest to the heat source.

Moritz and Henriques [1] first demonstrated on pigs and humans what was to become the classical inverse relation between the temperature and time required to produce a specific degree of thermal injury. Their data, which are replotted in Fig. 1, show that a burn wound of standard threshold severity can be produced by progressively decreasing temperatures as the duration of the thermal insult is logarithmically increased.

Numerous subsequent investigators have confirmed the same type of temperature-time response curve as presented by Moritz and Henriques. For example, Stoll and her co-workers [2] conducted detailed experiments on the interaction of burn time and temperature to cause specified injury levels in a human skin model. In a study preliminary to the development of the present analytical model, Ross and Diller [3] obtained similar results on a microvascular preparation in the hamster cheek pouch using very precise temperature measurement and control techniques. These data can be fit to a simple exponential function of the form

$$t = t_o \mathrm{EXP}[(T_o - T)/T_o] \tag{1}$$

or, in terms of dimensionless time, Γ, and temperature, Λ, as defined by

$$\Gamma = \frac{t}{t_o} \tag{2}$$

$$\Lambda = \frac{T}{T_o} \tag{3}$$

$$\Gamma = \mathrm{EXP}\,(1 - \Lambda) \tag{4}$$

where the reference time and temperature, t_o and T_o, reflect the relative intensity of the injury.

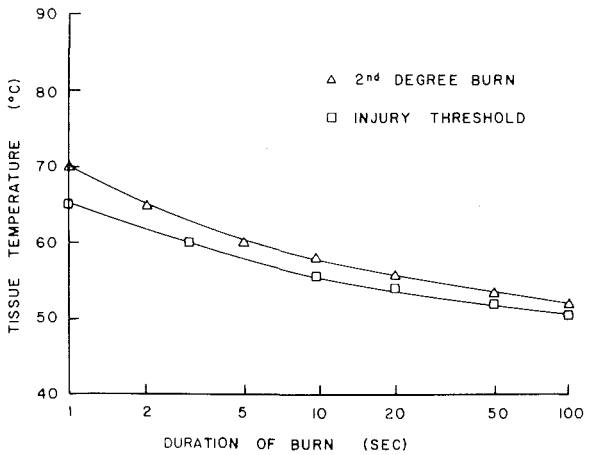

Fig. 1 Coupled interaction between temperature and exposure time requisite to produce a specified severity of burn injury. Replotted from [1].

Contributed by the Bioengineering Division for publication in the JOURNAL OF BIOMECHANICAL ENGINEERING. Manuscript received by the Bioengineering Division, September 10, 1982; revised manuscript received April 25, 1983.

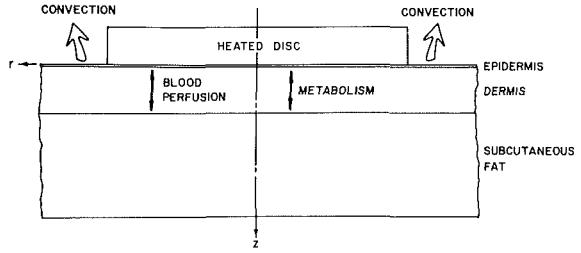

Fig. 2 Cylindrically symmetric cross-sectional geometry of skin model and heating source used in the burn injury simulation. Natural convection occurs from the skin to air peripheral to the source during the burn and over the entire surface for the postburn period.

The consistency of the data among numerous experimental protocols indicates that it should be possible to predict the extent of a burn wound using an appropriate analytical model. To be effective, such a model should incorporate parameters to account for thermal boundary conditions during a burn, constitutive and physiological properties of skin, and a criterion to define thresholds for the levels of injury.

Henriques and Moritz [4] were the first to propose a successful analytical model for thermal injury to skin. The transient temperature distribution was described in terms of the standard one-dimensional heat conduction equation

$$\frac{\partial T}{\partial t} = \frac{k}{\rho c}\frac{\partial^2 T}{\partial x^2} \tag{5}$$

They considered boundary conditions for conduction, convection, and radiation sources, coupled with the conduction of heat within the skin.

Subject to these boundary conditions, analytic solutions for equation (5) were obtained which describe temperatures in the affected tissue as a function of time and position. As part of the thermal injury model, Henriques and Moritz [4] devised a damage function which has subsequently been used quite widely. With this injury function, the cumulative damage incurred during a burn can be predicted. Thus, the simulation of a thermal burn in this model requires two computational steps; first, the transient temperature field must be determined for the boundary value problem of interest, and second, the thermal data must be applied to the evaluation of the damage rate function.

In deriving a damage function for burns, Henriques and Moritz [4] assumed that the governing biochemical processes could be depicted in terms of an Arrhenius-type relationship.

$$\kappa = \mathrm{A}\exp\left[-\frac{\Delta E}{RT}\right] \tag{6}$$

A is described as the frequency factor and κ as a second-order reaction rate constant. In their analysis the term Ω was used to denote an arbitrary degree of tissue injury, and the rate of production of injury was given by the damage rate function

$$\frac{d\Omega(x,t)}{dt} = \mathrm{A}\exp\left[-\frac{\Delta E}{RT(x,t)}\right] \tag{7}$$

The total injury, Ω, at any point in the tissue is obtained by integrating the damage rate function over the entire burn period, using the corresponding local transient temperature history, so

$$\Omega(x) = \mathrm{A}\int_o^t \exp\left[-\frac{\Delta E}{RT(x,t)}\right]dt \tag{8}$$

The function was quantified by Henriques to identify various injury thresholds. A value of $\Omega = 0.53$ was used to define the minimum conditions to obtain irreversible epidermal injury, whereas at $\Omega = 10^4$ complete transepidermal necrosis occurred. Thus, based on an evaluation of the local temperature history, and by applying equation (8), an estimate of the severity of burn injury can be made as a function of skin depth and radial position.

Subsequent to the work of Henriques and Moritz, their approach to modeling was adopted by other investigators to predict burn injury under various specific conditions of thermal insult. Significant among these studies are those by Buettner [5], Stoll and co-workers [6–8], Mainster, et al. [9], and Takata [10]. Within the past decade burn modeling has been accomplished by numerical analysis using finite difference techniques to take advantage of the capability of solving problems that are intractable analytically.

Mathematical Model

In the present study a two-dimensional rotationally symmetric temperature field in cylindrical coordinates was prescribed. The model simulates a physical process consisting sequentially of epidermal surface heating from a solid cylidnrical disk 1 cm in diameter for a specified time and temperature, followed by exposure to ambient air characterized by a natural convection boundary condition. A planar section of the physical system is shown in Fig. 2.

A number of assumptions were necessary in order to specify the details of the model, including:

1 No interfacial thermal resistance exists between the source and the tissue surface. As a result, the epidermal surface instantaneously assumes and remains at the temperature of the burning source throughout the duration of

Nomenclature

A = frequency factor in Arrhenins equation (6) (1/s)
B = Biot modulus defined by equation (15)
c = specific heat of tissue (J/kg.K)
ΔE = activation energy (J/kmol)
k = thermal conductivity (W/m.K)
q = metabolic heat generation rate (W/m^3)
r = radial coordinate (m)
$\bar{r}$ = dimensionless radial position defined by equation (15)
R = gas constant (J/kmol.K)
t = time (s)
T = temperature (C)
w = blood perfusion rate (L/s)
x = cartesian coordinate (m)
z = axial coordinate (m)
$\bar{z}$ = dimensionless axial position defined by equation (15)
α = thermal diffusivity (m^2/s)
Γ = dimensionless time defined by equation (2)
η = dimensionless metabolic heat generation defined by equation (15)
θ = dimensionless temperature defined by equation (25)
ζ = dimensionless temperature defined by equation (23)
κ = reaction rate factor (1/s)
Γ = dimensionless temperature defined by equation (3)
ρ = density (kg/m^3)
τ = dimensionless time defined by equation (15)
Υ = dimensionless temperature defined by equation (15)
ϕ = dimensionless blood perfusion rate defined by equation (15)
Ω = cumulative damage

Subscripts

a = arterial
b = blood
i = initial
o = reference value
s = source
∞ = ambient

application. The boundary condition is thereby specified by the source temperature along this portion of the epidermis.

2 The tissue is assumed to be isotropic and homogeneous within the individual layers of epidermis, dermis and subcutaneous fat. All three layers are of constant thickness, i.e., epidermis-75μm, dermis-1.5mm, and fat-3.425mm. In lieu of specific data to the contrary, all property values within each tissue type are considered constant and uniform, not varying with either temperature or position. Temperatures and heat fluxes are continuous at tissue interfaces.

3 Blood perfusion is significant only in the dermal layer where it is uniform in time and position. Thus, the perfusion term is unaltered even during the period of maximum burn intensity. This assumption represents an undeniable compromise with physiological reality in which it is well established that extreme hyperthermia elicits increased vascular permeability and/or stasis [2, 11]. Nonetheless, the assumption is made in the present context in order to provide the opportunity to simulate the relative influence of blood perfusion on the temperature field, and since specific data amenable to inclusion in the model is not available.

4 Metabolic heat generation is zero in the epidermis and subcutaneous fat and is negligible in the dermis in comparison to the other energy fluxes involved.

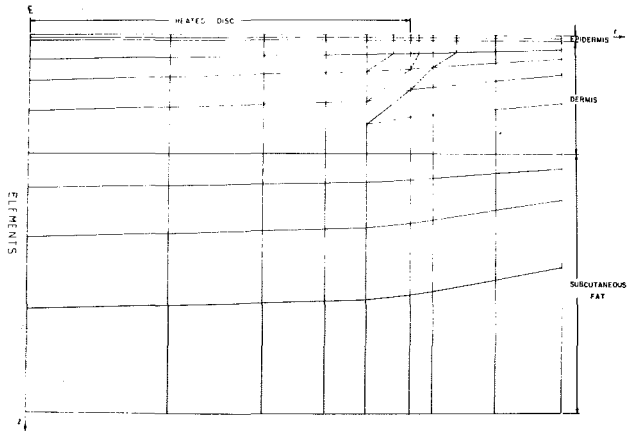

Fig. 3 Finite element grid network approximating a symmetric half-cross section of cylindrical skin burn model defined in Fig. 2

5 No phase change occurs in the tissue, although temperatures high enough to produce boiling have been observed in some burn experiments involving high local heat fluxes [1, 12, 13]. Again, the details of this process are unclear and not substantiated by data which could be used in the present model. The temperatures simulated in this study are confined to values below the range for which boiling would be expected.

6 During application of heat the epidermal surface peripheral to the hot contact area experiences natural convective heat transfer with ambient air at 298K. Subsequent to the removal of the heating disk the entire epidermal surface is convectively cooled by the ambient air.

The transient temperature distribution within the model tissue system is described mathematically by the standard bioheat transfer equation [14, 15] as

$$\frac{\partial T}{\partial t} = \alpha\left(\frac{\partial^2 T}{\partial r^2} + \frac{1}{r}\frac{\partial T}{\partial r} + \frac{\partial^2 T}{\partial z^2}\right) + \frac{\rho_b c_b w_b}{\rho c}[T_a - T] + \frac{q}{\rho c} \quad (9)$$

The convective term describes the heat transport between the tissue and microcirculatory blood perfusion, which is assumed to be distributed homogeneously and isotropically within the dermis. Internal heat generation is due to metabolism.

The initial and boundary conditions for this problem are established as follows. The entire tissue system is in an initial uniform isothermal state at $T_i = 34°C$. Temperatures and heat fluxes are continuous at tissue interfaces, and the radial temperature gradient is zero along the centerline of the system due to geometric and thermal symmetry. Axial and radial gradients are taken as zero along boundaries which are deep within the tissue and at large radii, respectively, since the effects of the heating source diminish rapidly at large distances. These conditions are stated accordingly as

$$T(r,z,0) = T_i \quad (10)$$

$$T(r,0,t) = T_s \text{ for } 0 \le r \le r_s \text{ and } 0 \le t \le t_s \quad (11a)$$

$$-k\frac{\partial T(r,0,t)}{\partial z} = h[T(r,0,t) - T_\infty] \text{ for } \begin{cases} r_s < r & 0 \le t \le t_s \\ 0 \le r & t_s \le t \end{cases} \quad (11b)$$

Table 1 Model parameter values

Symbol	Parameter	Units	Value range	Reference
A	Frequency factor in damage integral	1/s	3×10^{98}	5
c_b	Specific heat of blood	j/kg•s	3.3×10^{3}	25
ΔE	Activiation energy in damage integral	k/k mol	6.3×10^{8}	5
h	Convective heat transfer coefficient between skin and air or water	W/m^2•K	73,500	26
k	Thermal conductivity of skin	W/m•K		5,10,25
	(*a*) Epidermis		2.1×10^{-1}	
	(*b*) Dermis		3.7×10^{-1}	
	(*c*) Subcutaneous		1.6×10^{-1}	
q	Metabolic heat generation	W/m^3	0	
r_s	Radius of heating disk	m	5×10^{-3}	
r_{max}	Maximum radius in finite element grid	m	7×10^{-3}	
t_s	Duration of heating insult	s	15	
T_a	Temperature of arterial blood	K	310	
T_i	Initial tissue temperature	K	307	
T_s	Temperature of heating disk	K	363	
T_∞	Temperature of ambient air	K	298	
w_b	Dermal blood perfusion rate	mL blood/mL tissues	2.4×10^{2}	27-29
α	Thermal diffusivity of skin	m^2/s		5,10,25
	(*a*) Epidermis		0.66×10^{-7}	
	(*b*) Dermis		1.3×10^{-7}	
	(*c*) Subcutaneous		0.81×10^{-7}	
ρ_b	Density of blood	kg/m^3	1.1×10^{3}	30
ΔZ	Thickness of tissue layer	m		11
	(*a*) Epidermis		0.075×10^{-3}	
	(*b*) Dermis		1.500×10^{-3}	
	(*c*) Subcutaneous		3.425×10^{-3}	

$$\frac{\partial T(0,z,t)}{\partial r} = 0 \tag{12}$$

$$\frac{\partial T(r,\infty,t)}{\partial z} = 0 \tag{13}$$

$$\frac{\partial T(\infty,z,t)}{\partial r} = 0 \tag{14}$$

and the boundary conditions (13) and (14) which are appropriate for an infinite medium are imposed on the remote finite boundaries.

The boundary value problem defined by equations (9)-(14) may be restated in dimensionless terms by introducing the following set of parameters.

$$\tau = \frac{\alpha t}{r_s^2}; \Upsilon = \frac{T - T_a}{T_i - T_a}; \bar{z} = \frac{z}{r_s}; \bar{r} = \frac{r}{r_s} \tag{15}$$

$$\phi = \frac{\rho_b c_b}{k} r_s^2 w_b; \eta = \frac{q}{k} \frac{r_s^2}{(T_i - T_a)}; \mathrm{B} = \frac{h r_s}{k}$$

Substituting yields

$$\frac{\partial \Upsilon}{\partial \tau} = \frac{\partial^2 \Upsilon}{\partial \bar{r}^2} + \frac{1}{\bar{r}} \frac{\partial \Upsilon}{\partial \bar{r}^2} - \phi \Upsilon + \eta \tag{16}$$

$$\Upsilon(\bar{r},\bar{z},0) = 1 \tag{17}$$

$$\Upsilon(\bar{r},0,\tau) = \Upsilon_S \text{ for } 0 \le \bar{r} \le 1 \; 0 \le \tau \le \tau_s \tag{18a}$$

$$\frac{\partial \Upsilon(\bar{r},0,\tau)}{\partial \bar{z}} = \mathrm{B}[\Upsilon_\infty - \Upsilon(\bar{r},0,\tau)] \text{ for } \left\{ \begin{array}{ll} 1 < \bar{r} & 0 \le \tau \\ 0 \le \bar{r} & \tau_s \le \tau \end{array} \right\} \tag{18b}$$

$$\frac{\partial \Upsilon(0,\bar{z},\tau)}{\partial \bar{r}} = 0 \tag{19}$$

$$\frac{\partial \Upsilon(\bar{r},\infty,\tau)}{\partial \bar{z}} = 0 \tag{20}$$

$$\frac{\partial \Upsilon(\infty,\bar{z},\tau)}{\partial \bar{r}} = 0 \tag{21}$$

with the constraint that Υ and $k\,\partial\Upsilon/\partial z$ are continuous at tissue interfaces.

Numerical Model

A two-dimensional finite element program [16] was used to solve the axisymmetric equation (16) and thereby simulate the transient temperature field produced in the skin. The finite element method [17-18] is a modeling technique which offers many advantages over the more standard finite difference methods for solving heat transfer problems in biomedical applications. Although the finite element method has been used for many years in stress analysis problems, it has only recently been applied for modeling of biomedical heat transfer [20-24]. In the finite element method, the region of interest is divided into small regions, or elements. These regions are usually three or four-sided shapes which may have curved boundaries. Different material properties may be assigned to each element. The differential equation (16) is solved in an average or integrated sense over each element and the boundary conditions are satisfied in an averaged sense over each element edge which lies on the boundary. The finite element method can accommodate prescribed temperature, heat flux, or convective-type boundary conditions without a loss of accuracy near the boundary, and it automatically imposes continuity of temperature fields and heat flux at all element interfaces. Hence, temperatures and fluxes are continuous at intermaterial boundaries. A Crank-Nickolson time stepping method was used, and it is well known that the numerical technique used here is second order accurate in both time and space [19]. Thus, the finite element method can accurately resolve curved geometry and flux patterns, and is at least as accurate as the finite difference method. Small time steps and spatial elements were used, and initial verification of this model was done to insure numerical truncation errors did not significantly affect the calculated temperature fields.

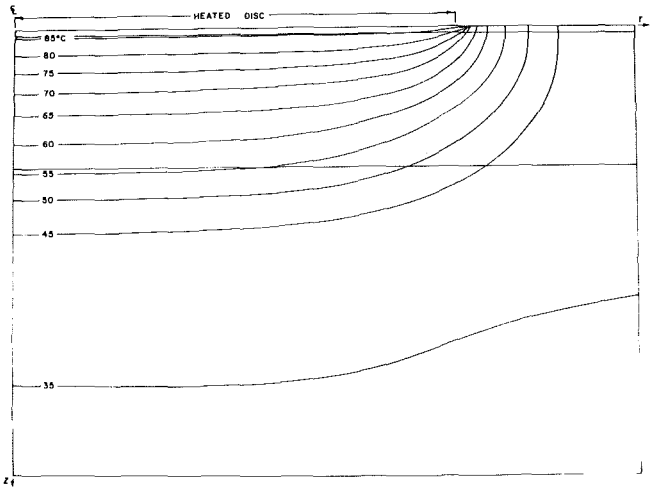

Fig. 4 Temperature profiles in the skin at the completion of a 90°C, 15-s burn protocol

Due to the inherent flexibility of the finite element method in handling a grid mesh of general geometry, it was possible to generate a nonlinear network emphasizing a high concentration of elements in the region near the heat source where the steepest thermal gradients were expected. A sample element grid layout is shown in Fig. 3. A composite system corresponding to Fig. 2 consisting of three parallel, unequal layers of epidermal, dermal, and subcutaneous fatty tissue was used.

The development of injury was predicted from the calculated temperature-time history by using the Henriques damage function.

$$\frac{d\Omega(\bar{r},\bar{z},\tau)}{d\tau} = \mathrm{A} \exp\left[- \frac{\overline{\Delta E}}{\Upsilon + \zeta} \right] \tag{22}$$

where dimensionless activation energy and temperature terms are defined as

$$\overline{\Delta E} = \frac{\Delta E}{R(T_i - T_a)}, \zeta = \frac{T_a}{T_i - T_a} \tag{23}$$

At each time step in the finite element solution the two-dimensional thermal field was used to determine the local rate of injury. Cumulative damage accrued during the thermal insult was then determined as

$$\Omega(\bar{r},\bar{z},\tau) = \int_o^\tau \frac{\partial \Omega}{\partial \tau} d\tau$$

$$= \mathrm{A} \int_o^\tau \exp\left[- \frac{\overline{\Delta E}}{\Upsilon(\bar{r},\bar{z},\tau) + \zeta} \right] d\tau$$

$$= \Omega(\bar{r},\bar{z},\tau - \Delta\tau) + \frac{\partial \Omega(\bar{r},\bar{z},\tau)}{\partial \tau} \Delta\tau \tag{24}$$

where $\Delta\tau$ defines the current time increment.

The effects of various thermal and physiological parameters on the extent and severity of tissue burn injury were studied. Numerical values of individual parameters as used in the study are presented in Table 1.

Results

Two-dimensional temperature and damage integral contours were obtained for various burn and postburn protocols

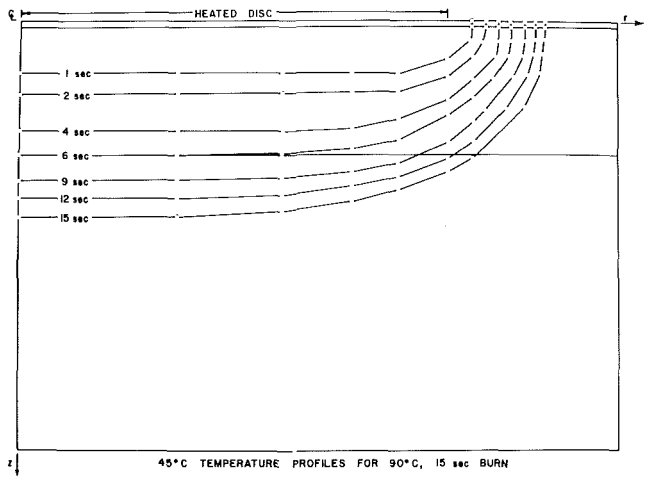

Fig. 5 Progression of 45°C isotherms into the skin at specific times during the 90°C, 15-s burn protocol

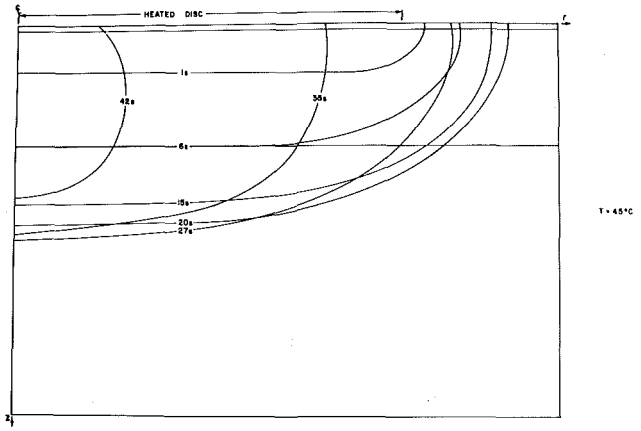

Fig 6 Locii of 45°C isotherms subsequent to completion of a 90°C, 15-s burn for natural convection heat transfer to air over the entire skin surface. Time is measured from the initiation of the burn process. All tissue temperatures were lower than 45°C at 45 s (30-s postburn)

to aid in illucidation of the physicochemical progression of the injury process. Examples of these contours are presented as follows.

In Fig. 4, a typical temperature field as shown which has developed in the tissue at the completion of a 90°C, 15-s thermal insult. As expected, the isotherms lie parallel to the skin under the centermost portion of the heating disk and the axial temperature gradient decreases with distance from the skin surface. In contrast, at the edge of the disk the isotherms are skewed drastically to be normal to the surface, and the maximum temperature gradient in the entire system occurs in the radial direction. For this protocol the 45°C isotherm, which is approximately the threshold temperature for tissue damage, penetrates completely through the skin layers into the subcutaneous fat. The 45°C isotherm also extends to a radial position identified by $\bar{r}=1.23$ beyond the edge of the heating disk.

The progression of the temperature field in time for the above thermal protocol is shown in Fig. 5 where the 45°C isotherm is plotted at incremental times during the burn. It is apparent from the one second isotherm that the initial movement of the temperature field into the underlying tissue is very rapid. Also, complete penetration through the dermal layers is achieved within only 6 s. The 45°C isotherm is also shown in Fig. 6 for times subsequent to the removal of the heating disk at 15 s; at which time the entire skin surface is

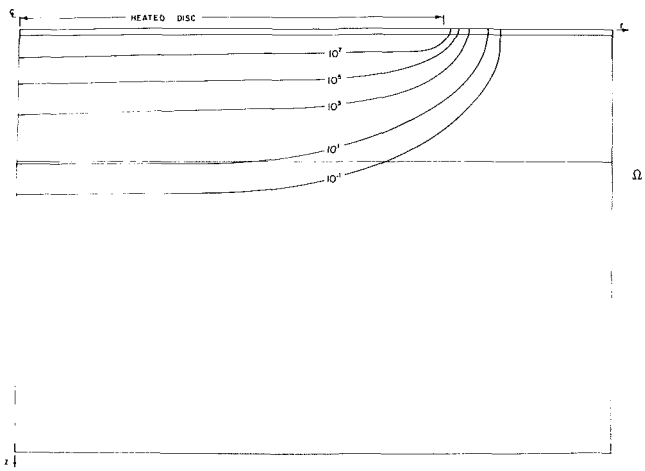

Fig. 7 Damage integral profiles at completion of a 90°C, 15-s burn protocol

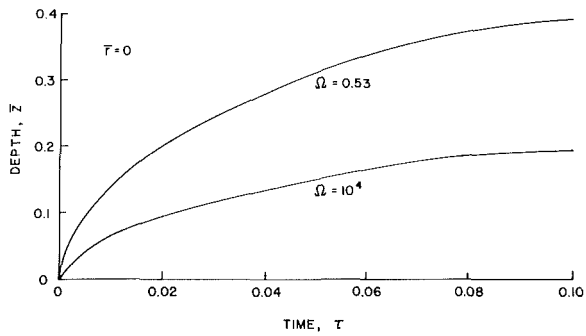

Fig. 8 Depth of maximum penetration of threshold and 3rd degree injuries into skin tissue as a function of dimensionless axial position and time

exposed to a free convection boundary condition with ambient air at 295°C. Thermal inertia affects within the tissue are readily apparent with the initiation of cooling. Elevated temperatures continue to move further into the tissue for more than 20 s after removal of the disk, even while the skin surface is being cooled. Thus, although the burning source is removed the damage interface progresses to a greater tissue depth. This effect is consistent with data reported previously by Stoll [6]. Eventually, more than 30 s of exposure time are required for all the tissue in the affected area to be cooled below the threshold injury temperature of 45°C.

Final damage integral contours produced at the termination of the foregoing thermal protocol are presented in Fig. 7 for a range of eight orders of magnitude between 10^{-1} and 10^7. According to Henriques' criterion of Ω equal to 0.53, 1.0, and 10^4, corresponding, respectively, to injury threshold, second, and third-degree burns, this predicted injury is in general agreement with available experimental data. For example, the 90°C, 15 s protocol is known to produce a full thickness, third degree wound on skin of average depth, such as that of the thigh or back [31]. Correspondingly, in Fig. 7 at the termination of the burn process the third degree wound threshold has penetrated to just below the dermal layer, representing a full thickness burn. The radial extent of second and third-degree injury are predicted to be confined to $\bar{r}=1.12$ and $\bar{r}=1.05$, respectively.

The axial penetration of the wound during the thermal insult process and post burn cooling period at $\bar{r}=0$ are illustrated in Fig. 8. The maximum tissue depth to which threshold and third degree burns have progressed is shown as a function of dimensionless time. Although the greatest injury depth occurred the centerline directly beneath the heating disk ($\bar{r}=0$), there was only a few percent falloff in penetration for

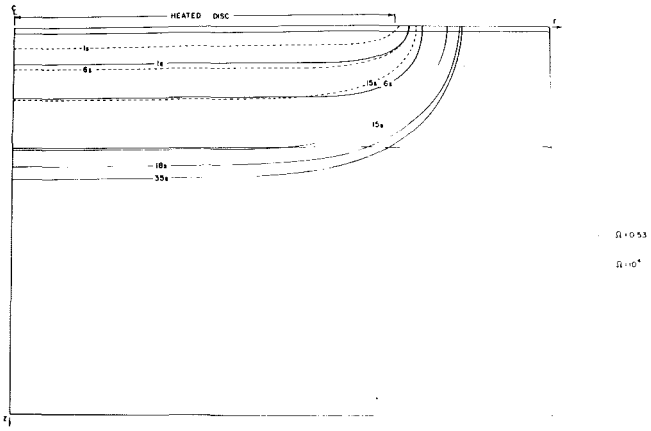

Fig. 9 Damage integral profiles for threshold and third-degree injuries during and subsequent to exposure to the heated disk

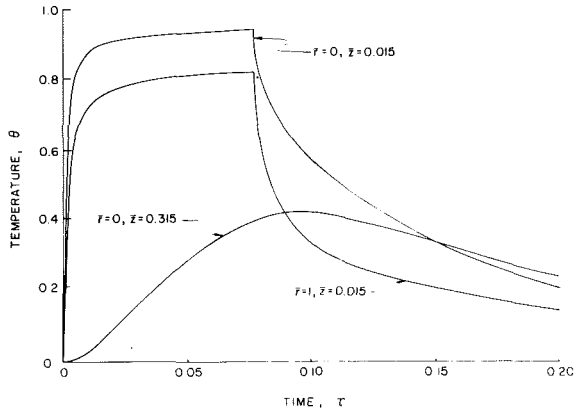

Fig. 10 Temperature profiles at three representative points in the skin during 90°C, 15-s burn protocol. $\bar{r}=0$ is the centerline of the system, $\bar{r}=1$ is the edge of the heat source, $\bar{z}=0.015$ is the epidermis-dermis interface, and $\bar{z}=0.315$ is the dermis-subcutaneous fat interface

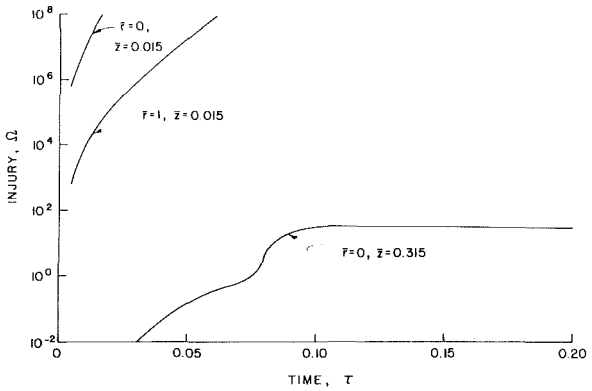

Fig. 11 Transient damage integral functions for the thermal histories defined in Fig. 10

$\bar{r} \leq 0.8$, as shown in Fig. 7. Consequently, the extent of burn injury is nearly maximal for the central 2/3 of the skin area beneath the heating disk. The penetration ratio of third degree to threshold burns at any given time is about 47 percent; thus, the volume of tissue subjected to third-degree injury is approximately 1/3 of that for threshold injury. The time progression of injury in the tissue may also be inferred from Fig. 8. For example, at any selected value of $\bar{z}$, the time required to produce a third-degree burn in comparison to a threshold burn is greater by a factor of approximately 4.3. Clearly, the duration of burn exposure plays a significant role in determining the extent of tissue injury at any skin depth. Inspection of Fig. 8 indicates that at a moderately high surface temperature of 90°C, even after a very long burn duration of 15 s ($\tau = 0.078$), the movement of the threshold injury interface into the tissue is proceeding at a finite rate. The asymptotic limit at which a steady state injury profile would be achieved was not computed for the present boundary conditions; however, it is readily apparent that burn periods considerably longer than are encountered in a majority of injuries are required to establish the stationary thermal field and are therefore of little practical relevance.

The increment in wound severity accrued after removal of the heating source is demonstrated in Fig. 9. Curves of $\Omega = 0.53$ and 10^4 are plotted at incremental times from the beginning of the burn until a final steady state is achieved at approximately 20-s post burn. There is not a significant change in the third-degree injury profile following removal of the heated disk. However, it is apparent from this simulation that a significant portion of the threshold level injury may occur after termination of the burn insult, which is in agreement with the earlier prediction by Stoll [7].

The fact that the burn injury process may continue for some time after termination of the thermal insult is again illustrated in Fig. 10, in which profiles of the dimensionless temperature are drawn at three different tissue locations: 1) at the dermis-epidermis interface on the centerline ($\bar{r}=0$), 2) at the dermis-epidermis interface directly beneath the edge of the heating source ($\bar{r}=1$), and 3) at the dermis-subcutaneous fat interface on the centerline ($\bar{r}=0$). This data is for the 90°C, 15-s burn. θ is defined by

$$\theta = \frac{T - T_i}{T_s - T_i} \tag{25}$$

where T_s is the temperature of the heat source. All three profiles exhibit significant distinctions for both the heating and cooling phases. At large values of $\bar{z}$, the deep tissue profile shows a time lag in response to alterations in surface boundary conditions, due to thermal inertia of overlying epidermal and dermal layers. The responses in the deep tissue profiles are very smooth, and they do not have the abrupt changes which are characteristic of tissue near the surface. Radial position effects are apparent in that heating rate is lower, the cooling rate is higher, and the temperature at all times is lower under the edge of the disk than at the center because of the proximity to peripheral convective heat transport to the cooler environment. Reference to Figs. 4 and 5 indicates there is very little radial variation in the temperature profile for values of $\bar{r}$ less than 0.75. Thus, influence of the peripheral convective cooling is propagated only a relatively short distance in the tissue underlying the heat source.

In contrast to the differences pointed out in the foregoing, there is an important similarity among the curves shown in Fig. 10, that being a substantial time delay after removal of the heat source until tissue temperatures return to values below which the injury rate becomes negligible ($\theta \leq 0.30$). The threshold temperature for burn injury is on the order of 44°C [2], which corresponds to $\theta = 0.18$ for the present protocol. Thus, the fraction of exposure time to suprathreshold temperatures which occurs after completion of the thermal insult is 53 percent for $\bar{r} = 1$, $\bar{z} = 0.015$, 64 percent for $\bar{r} = 0$, $\bar{z} = 0.015$, and 78 percent for $\bar{r} = 0$, $\bar{z} = 0.315$. Clearly, the injury process continues after removal of the heat source. However, of more importance is the increase in the damage integral which is exponentially proportional to the temperature differential above the threshold temperature, equation (22). The time history of the damage integrals at these three points is shown in Fig. 11. The burn integrals are calculated for the three temperature profiles in Fig. 10 and plotted for values of between 10^{-2} and 10^8. The integrals at $\bar{z} = 0.015$ very rapidly exceed the spectrum of values com-

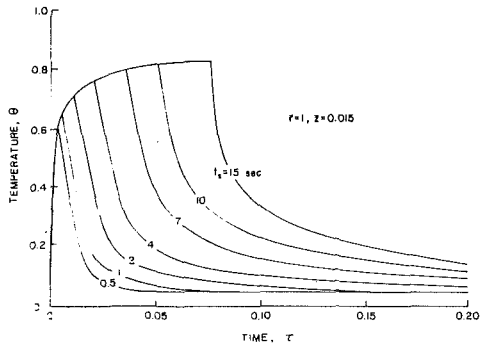

Fig. 12 Temperature profiles at the base of the epidermis directly under the edge of a 90°C heating disk for various durations of exposure

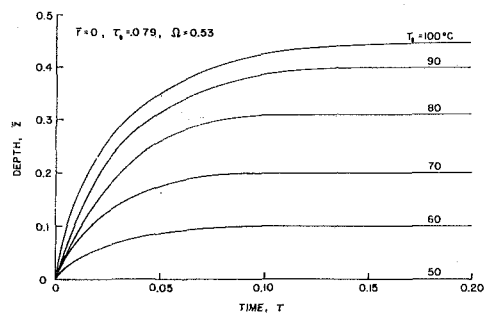

Fig. 13 Penetration of threshold injury (Ω = 0.53) for at $\bar{r} = 0$ for 15-s (τ_S = 0.079) burns at the indicated temperatures

puted, and for which experimental data is available, whereas the Ω at $\bar{z} = 0.315$ may be followed for the duration of the simulation. Since a finite time is required for changes in boundary conditions to be propagated through the skin to the base of the dermis, there exists an initial delay after application of the heating disk before any appreciable injury occurs. For this point Ω reaches a value of 10^{-2} at approximately the same time that the local temperature becomes 44°C. As the tissue temperature is raised the rate of increase of Ω also increases until a maximum occurs, corresponding to the peak temperature attained. As the tissue temperature decreases, the rate at which Ω increases is also lowered, resulting in an inflection point on the curve. However, a substantial portion of the injury is clearly seen to occur for times greater than τ_s. The ratio of Ω at large τ to τ_s is approximately 75:1 for the present case indicating that nearly all of the deep tissue injury occurs following termination of the insult process. The ratio decreases for tissue nearer to the surface due to a more rapid response to changes in the boundary conditions.

Finally, the effects of variations in the burn temperature and duration were simulated. Temperature profiles for exposure to a 90°C disk for heating periods between 0.5 and 15 s are shown in Fig. 12. As would be expected, as the time of exposure to the heating disk is increased, the length of time that the tissue temperatures are above the injury threshold value of $\theta = 0.18$ after heat removal is also increased. There is nearly a 1:1 correspondence between the length of heating and the total time spent at $\theta \leq 0.18$. However, as the heating time becomes longer, a larger fraction of the total time occurs at elevated temperatures, i.e., $d\theta/dt$ decreases, and the injury rate $d\Omega/dt$ increases. Therefore, the injury function Ω grows exponentially with time of exposure. In general, the ratio of exposure times required to produce threshold (Ω = 0.53) and third degree ($\Omega = 10^4$) injuries at a given location within the tissue is approximately 4:1 (see also Fig. 8).

The deepest penetration of the threshold injury interface (Ω = 0.53) into the tissue is illustrated in Fig. 13 for burns of 15 s at disk temperatures varying between 50 to 100°C. Temperatures in excess of 100°C were not simulated in order to avoid complexities associated with modeling thermodynamic and mechanical aspects of the liquid-vapor phase change. The curves all follow the same pattern of development, with penetration increasing with disk temperature. The model shows no injury at a disk temperature of 50°C. At 60°C the injury threshold has moved well into the dermis and 80°C is adequate to reach the fat layer. The final depth of maximum penetration is reached at a later time for high disk temperatures since the interface is at a larger $\bar{z}$ and is therefore less responsive to surface effects. Thus, burns at higher temperatures may present greater opportunity for therapeutic manipulation of the post-burn thermal protocol to reduce the final degree of injury. This possibility is discussed in a companion paper in terms of various post-burn cooling regimens [32].

Conclusion

Although the physiological response to burns involves complicated and coupled reactions, even simple techniques of heat transfer analysis may contribute substantially to the understanding of the burn wound process and how it may be treated. Quantitative analysis can be used to predict the extent and severity of injury due to prescribed environmental heating and cooling factors, and to access the physiological response to a given thermal insult. Recent advances in digital computing capacity and in development of finite element analysis codes have allowed successful analysis of heat transfer in complex geometrics and hold the promise of providing more powerful and generally useful techniques of heat transfer analysis as applied to burn injury. For example, the finite element method is currently being used to analyze the effects of nonuniform perfusion of blood at variable rates through the skin [33].

References

1 Mortiz, A. R., and Henriques, F. C., "Studies of Thermal Injury. II. The Relative Importance of Time and Surface Temperature in the Causation of Cutaneous Burns," *The American Journal of Pathology*, Vol. 23, 1947, pp. 695-720.

2 Stoll, A. M. "Heat Transfer in Biotechnology," *Advances in Heat Transfer*, Vol. 4, eds., by J. P. Hartnett and T. F. Irvine, Jr., Academic Press, New York, 1969, pp. 65-141.

3 Ross, D. C., and Diller, K. R., "An Experimental Investigation of Burn Injury in Living Tissue," ASME *Journal of Heat Transfer*, Vol. 98, 1976, pp. 292-296.

4 Henriques, F. C., and Moritz, A. R., "Studies of Thermal Injury. I. The Conduction of Heat to and Through Skin and the Temperatures Attained Therein. A Theoretical and an Experimental Investigation," *The American Journal of Pathology*, Vol. 23, 1947, pp. 531-549.

5 Buettner, K., "Effects of Extreme Heat and Cold on Human Skin. I. Analysis of Temperature Changes Caused by Different Kinds of Heat Application," *Journal of Applied Physiology*, Vol. 3, 1951, pp. 691-702.

6 Stoll, A. N., and Green, L. C., "Relationship Between Pain and Tissue Damage Due to Thermal Radiation," *Journal of Applied Physiology*, Vol. 14, 1959, pp. 373-382.

7 Stoll, A. M., "A Computer Solution for Determination of Thermal Tissue Damage Integrals form Experimental Data," *Institute of Radio Engineers Transactions on Medical Electronics*, Vol. 7, 1960, pp. 355-358.

8 Weaver, J. A., and Stoll, A. M., "Mathematical Model of Skin Exposed to Thermal Radiation," *Aerospace Medicine*, Vol. 40, 1969, pp. 24-30.

9 Mainster, M. A., White, T. J., Tips, J. H., and Wilson, P. W., "Transient Thermal Behavior in Biological Systems," *Bulletin of Mathematical Biophysics*, Vol. 32, 1970, pp. 303-314.

10 Takata, A. N., Zaneveld, L., and Richter, W., "Laser-Induced Thermal Damage of Skin," SAM-TR-77-38, USAF School of Aerospace Medicine, 1977, pp. 1-159.

11 Krizek, T. J., Robson, M. C., and Wray, R. C., Jr., "Care of the Burned Patient," *The Management of Trauma, Second Edition*, eds., W. F. Ballinger, R. B. Rutherford, and G. D. Zuidema, W. B. Saunders Co., Philadelphia, 1973, pp. 650—718.

12 Stoll, A. M. Piergallini, J. R., and Chianta, M. A., "Rocket Plume Burn Hazard," *Aviation, Space, and Environmental Medicine*, Vol. 51, 1980, pp. 480-484.

13 Bellina, J. H., and Seto, Y. J., "Pathological and Physical Investigations

into CO_2 Laser-Tissue Interactions with Special Emphasis on Cervical Intraepithelial Neoplasm," *Lasers in Surgey and Medicine*, Vol. 1, 1980, pp. 47-69.

14 Pennes, H. H., "Analysis of Tissue and Arterial Blood Temperatures in the Resting Human Forearm," *Journal of Applied Physiology*, Vol. 1, 1948, pp. 93-122.

15 Cravalho, E. G., Fox, L. R., and Kan, J. C., "The Application of the Bioheat Equation to the Design of Thermal Protocols for Local Hyperthermia," *Annals of the New York Academy of Sciences*, Vol. 335, 1980, pp. 86-97.

16 Hayes, L. J., "A Users Guide to PARAB: A Two-dimensional Linear Time-dependent Finite Element Program," TICOM Report No. 80-10, The University of Texas at Austin, 1980, pp. 1-40.

17 Becker, E. B., Carey, G. F., and Oden, J. T., "Finite Elements: An Introduction, Vol. 1," Prentice-Hall, New York, 1981.

18 Zienkiewicz, O. C., *The Finite Element Method*, 3rd Edition," McGraw-Hill, New York, 1977.

19 Douglas, J., and Dupont, T., "Galerkin Methods for Parabolic Equations," *Journal of Numerical Analysis*, SIAM, Vol. 7, 1970, pp. 575-626.

20 Bald, W. B., "New Technique for Determining Thermal History and Concentration Gradients in Biological Specimens During Cryopreservation, Cryosurgery and Ultrastructural Studies," *Cryoletters*, Vol. 2, 1981, pp. 201-206.

21 Peskin, C. S., "Computer Testing of Artificial Heart Values,"invited lecture, SIAM Fall Meeting, Houston, 1980.

22 Rubinsky, B., and Cravalho, E. G., "A Finite-Element Method for the Solution of One-dimensional Phase Change Problems," *International Journal of Heat and Mass Transfer*, Vol. 12, 1980, pp. 1587-1589.

23 Hayes, L. J., and Diller, K. R., "Comparison of One- and Two-dimensional Finite Element Models for a Freezing Heart Process," *Proceedings SIAM Fall Meeting*, Houston, 1980.

24 Hayes, L. J., and Diller, K. R., "A Finite Element Model for the Exposure of a Composite Man with Distributed Internal Heat Generation to a Convective Subfreezing Environment," ASME Paper No. 81-WA/HT-52.

25 Bowman, H. F., Cravalho, E. G., and Woods, M., "Theory, Measurement, and Application of Thermal Properties of Biomaterials," *Annual Review of Biophysics and Bioengineering*, Vol. 4, 1975, pp. 43-80.

26 Incropera, F. P., and DeWitt, D. P., *Fundamentals of Heat Transfer*, Wiley, New York, 1981.

27 Guyton, A. C., *Textbook of Medical Physiology*, Third Edition, W. B. Saunders Co., Philadelphia, 1971.

28 Folkow, B., and Neil, E., *Circulation*, Oxford University Press, London, 1971.

29 Greenfield, A. D. M., "The Circulation Through the Skin," *Handbook of Physiology, 2, Circulation II*, 1963, pp. 1324-1351.

30 Wintrobe, M. M., *Clinical Hematology*, 7th Edition, Lea & Febiger, Philadelphia, 1975.

31 Bailey, B. N., Lewis, S. R., and Blocker, T. G., Jr., "Standardization of Experimental Burns in the Laboratory Rat," *Texas Reports of Biology and Medicine*, Vol. 20, 1961, pp. 20-29.

32 Diller, K. R., Hayes, L. J., and Baxter, C. R., "A Mathematical Model for the Thermal Efficacy of Cooling Therapy for Burns," *Journal of Burn Care and Rehabilitation*, Vol. 4, 1983, pp. 81-89.

33 Diller, K. R., and Hayes, L. J., "Analysis of Blood Perfusion Effects on Skin Burn Injury," submitted for publication to ASME JOURNAL OF BIOMECHANICAL ENGINEERING, 1983.